Science Bulletin 64 (2019) 1087–1094

Contents lists available at ScienceDirect

Science Bulletin

journal homepage: www.elsevier.com/locate/scib

Science Bulletin
www.scibull.com

Article

Efficient ternary organic solar cells based on a twin spiro-type non-fullerene acceptor

Lirong Wu [a,1], Lingchao Xie [b,c,1], Hanmin Tian [a], Ruixiang Peng [b], Jiaming Huang [b], Billy Fanady [b], Wei Song [b], Songting Tan [c], Wengang Bi [a,*], Ziyi Ge [b,*]

[a] School of Electronics and Information Engineering, Tianjin Key Laboratory of Electronic Materials and Devices, Hebei University of Technology, Tianjin 300401, China
[b] Ningbo Institute of Materials Technology and Engineering, Chinese Academy of Sciences, Ningbo 315201, China
[c] Key Laboratory of Environmentally Friendly Chemistry and Applications of Ministry of Education, College of Chemistry, Xiangtan University, Xiangtan 411105, China

ARTICLE INFO

Article history:
Received 29 April 2019
Received in revised form 31 May 2019
Accepted 5 June 2019
Available online 8 June 2019

Keywords:
Ternary organic solar cells
High efficiency
Photon harvesting
Charge transport
Energy transfer

ABSTRACT

A novel small-molecule (SM) acceptor DTF-IC is designed and synthesized in this work. The power conversion efficiency (PCE) of ternary OSCs increased up to 12.14% from 10.90% by incorporating 10 wt% of DTF-IC as second acceptors into the binary OSCs consisting of PBDB-T as donor and IT-M as acceptor. This was mainly due to the large increase in short-circuit current (J_{sc}) from 16.18 to 17.95 mA/cm^2, without any drop in the open-circuit voltage (V_{oc}) and fill factor (FF). The addition of DTF-IC enabled the donor and acceptor to form a distinct complementary absorption profile in the visible-light region, which boosted the photon harvesting in the range of 730–800 nm and consequently increased the J_{sc} of the ternary system by 11%. Moreover, there was an energy transfer between the two SM acceptors, favorable for enhancing charge separation and transfer as well as reducing charge recombination at PBDB-T:IT-M and PBDB-T:DTF-IC interface. Simultaneously, HOMO and LUMO energy levels of DTF-IC were lower than those of PBDB-T, but still higher than those of IT-M. Thus, DTF-IC is able to provide a cascading energy level with the host donor and acceptor which are beneficial for efficient charge transfer between the acceptors and facilitating exciton dissociation and carrier transport. Meanwhile, the highly crystalline DTF-IC as a third component can improve the crystallization process of the active layer while maintaining proper phase separation. This work proposes a novel idea for non-fullerene acceptors achieved via twin spiro-type structure modifying by indanone and provides a new direction for the selection of ternary solar cell materials.

1. Introduction

In recent years, the use of non-fullerene acceptors has led to the rapid development of organic solar cells with significantly improved efficiency [1–3]. The highest reported efficiency of single-junction device to date has exceeded 16% [4]. More researchers are working on synthesizing new molecular and optimizing device structures to improve photovoltaic performance [5–7]. Optimizing the active layer is one of the most important factors to improve the power conversion efficiency (PCE). However, due to the narrow absorption spectrum, high energy loss and low charge transfer efficiency of binary solar cells, the PCE of single-junction device is limited. Although the tandem device can make use of most photon, its structure is complicated. In contrast, the advantages of the ternary device are more prominent [8]. On the premise that the device fabrication process is not complicated, the suitable addition of the third component can boost the photon harvesting capability and play a role in energy transfer or charge transmission [9,10]. In some cases, the third component with relatively high crystallinity can also promote phase separation and achieve the ideal morphology of the active layer [11–13]. In addition, the high open-circuit voltage (V_{oc}) is very important for organic solar cells. Classic polymers could realize high V_{oc}, especially beyond 1.0 V. Zhou and co-workers [14] realized high V_{oc} of 1.02 V for P3HT-based organic solar cell using a benzotriazole-containing non-fullerene acceptor. A year later, they got a higher V_{oc} of 1.22 V by using a benzotriazole-containing nonfullerene acceptor end-capped with thiazolidine-2,4-dione [15]. In addition to the P3HT system, they also achieved high V_{oc} beyond 1.0 V based on J61 and J52-F [16,17]. In 2016, Zhan group [18] doped non-fullerene acceptor IDT-DPR-R as the third component into the P3HT:PCBM system. Since IDT-DPR-R with strong near-infrared

* Corresponding authors.
E-mail addresses: wbi@hebut.edu.cn (W. Bi), geziyi@nimte.ac.cn (Z. Ge).
[1] Lirong Wu and Lingchao Xie contributed equally to this work.

https://doi.org/10.1016/j.scib.2019.06.008
2095-9273/

absorption, the ternary device can significantly boost the photo harvesting. Many researchers also doped the third component into the classic PTB7-Th system over the years. For example, Wang et al. [19] added 3,9-bis (2-methylene-(3-(1,1-dicyanomethylene)-indanone)-5,5,11,11-tetrakis(4-hexylphenyl)-dithieno[2,3-*d*:2′,3′-*d*′]-s-indaceno[1,2-*b*:5,6-*b*′]-dithiophene (ITIC) into this system, which increased the V_{oc} due to the complementary energy levels. Similarly, Wang's group [11] introduced PFFBT4T-2OD into PTB7-Th:PCBM system, which promoted the energy transfer and optimized the blend film morphology, this showed PCEs of up to 10.72%. From the aspect of improving the morphology of blend film, a liquid crystalline small molecule BTR has been synthesized by Huang group [20]. They doped it into PTB7 system, which greatly improved the film morphology and consequently raised the power conversion efficiency to 11.4%. In the PBDB-T (poly [(2,6-(4,8-bis(5-(2-ethylhexyl)thiophen-2-yl)benzo[1,2-*b*:4,5-*b*′]dithiophene)-*co*-(1,3-di(5-thiophene-2-yl)-5,7-bis(2-ethylhexyl)-benzo[1,2-*c*:4,5-*c*′]dithiophene-4,8-dione)]) system, Hou group and Ge group [21] added the non-fullerene small-molecular ITCN ((2,2′-((5*E*,5′*E*)-5,5′-((5,5′-(4,4,9,9-tetrakis(5-hexylthiophen-2-yl)-4,9-dihydro-s-indaceno[1,2-*b*:5,6-*b*′]dithiophene-2,7-diyl)bis(4-(2-ethylhexyl)thiophene-5,2-diyl))bis(methanylylidene))bis(3-hexyl-4-oxothiazolidine-5,2-diylidene))dimalononitrile) as the third component to PBDB-T:IT-M, which widened the absorption spectrum and provided cascade energy levels, thus increasing the efficiency up to 12.16%. In terms of energy transfer, Nian et al. [22] used the acceptor P1 as a third component to form an energy transfer channel with the original acceptor, which improved the charge extraction. In terms of charge transfer, An et al. [23] doped N2200 as a third component into the ITIC, and effective mutual quenching could occur between the two acceptors, which facilitating the charge transfer process. Therefore, non-fullerene acceptors are more widely used as the third component due to their stronger absorption in the visible region and easier tuning of the lowest unoccupied molecular orbital (LUMO) energy level [2,24–26]. Addition of the third component must be compatible to the host binary solar cells so that the performance can be enhanced not only in terms of absorption spectrum, but also in terms of crystallinity as well as charge transport and collection. As a result, short-circuit current (J_{sc}) can be enhanced without reducing V_{oc} and destroying the film morphology of the active layer.

Here, a novel small-molecular acceptor DTF-IC was designed and synthesized (Fig. 1a). The end group of this small-molecular acceptor was indanone, and the blend morphology of the non-fullerene acceptor was controlled by side-chain engineering. The absorption peak of DTF-IC was found to be around 745 nm, which filled the gap in the weak part of the absorption spectrum. This broadened the absorption range of the active layer and enhanced the photon harvesting. Apart from the advantage of absorbing more sunlight, the absorption spectrum of DTF-IC highly overlaps with the PL spectrum of IT-M, indicating an effective energy transfer that occurred between the two acceptors. This is conducive for the extraction of internal DTF-IC excitons and effective charge separation at the PBDB-T:IT-M or PBDB-T:DTF-IC interface. Another important reason for the substantial increase in J_{sc} is that the addition of the third component forms an energy cascade, which enhanced charge transfer and reduced charge recombination. In this cascade model, the energy level of the third component is intermediate to the host donor and acceptor, which facilitated the transport process of holes to the anode and electrons to the cathode. These characteristics of the third component are all ded-

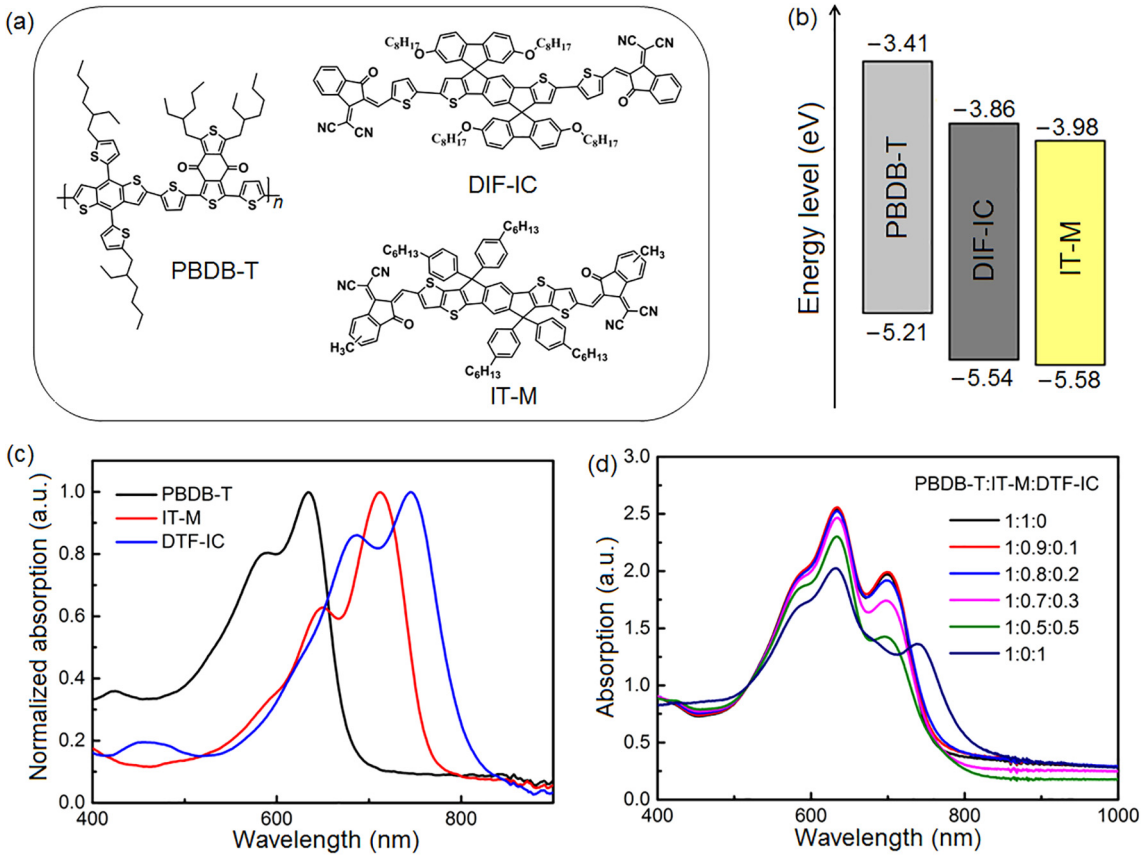

Fig. 1. (Color online) Chemical structures, energy levels and absorption spectra diagram. (a) Chemical structures and (b) energy levels of PBDB-T, DTF-IC and IT-M. (c) Normalized absorption spectra of neat films. (d) Absorption spectra of blend films with different DTF-IC contents.

icated to improve the J_{sc} of the solar cells. This was manifested by raising the J_{sc} of the PBDB-T:IT-M binary solar cell from 16.18 to 17.95 mA/cm^2. While the current was greatly increased, the fill factor (FF) did not drop due to the fused ring structure of DTF-IC that promoted a very strong crystallinity. Due to the high crystallinity, when it was doped into the PBDB-T:IT-M system as the third component [27,28], the domain purity and the coherence length were increased appropriately. This microstructure change in the mixed film could promote the phase separation between acceptors, which played a positive role in facilitating charge transport. Finally, 10 wt % DTF-IC was added to improve the efficiency of PBDB-T:IT-M from 10.9% to 12.14% (12% increment). This proved the potential of DTF-IC as second non-fullerene SM acceptor materials in ternary system.

2. Experimental

2.1. Materials and characterization

The *J-V* curve of the devices were measured by the instrument of Newport-Oriel Sol3A 450 W solar simulator, which could simulate the sunlight under the conditions of 100 mW/cm^2, AM 1.5G. The external quantum efficiency (EQE) spectra was measured by Newport-Oriel IQE 200, which was calibrated by a standard Si/Ge solar cell. In order to measure the thickness of different active layers, the computer controlled Dektak 150 Veeco was used. Dimension 3100 instrument (Vecco, USA) was used to scan the AFM images. PL spectra was measured with the instrument of FL3-111 (HORIBA, France) using the 712 nm lamp as the excitation source. Lambda 950 instrument (Perkin-Elmer, USA) was used to determine the Ultraviolet absorption spectrum.

2.2. Synthesis of DTFBT-1

Compound **1** (1.01 g, 0.72 mmol), compound **2** (0.79 g, 2.16 mmol) and Pd $(PPh_3)_4$ (40 mg, 0.070 mmol) were added into two-neck round-bottom flask. The flask was subjected to three successive cycles of vacuum followed by refilling with argon. Then, anhydrous toluene was added using a syringe. The Stille-coupling was carried out at 110 °C for 12 h. The organic layer was extracted with $CHCl_3$ (50 mL × 3) and dried over anhydrous $MgSO_4$. The raw product was obtained by using column chromatography on silica gel while petroleum ether:CH_2Cl_2 (v:v = 1:3) was treated as eluent. Finally, dark blue solid was precipitated with CH_3OH for purification. DTF-IC, Yield: 0.81 g, 72%. ^{1}HNMR (400 MHz, $CDCl_3$) δ (ppm): 8.73(s, 2H), 8.65 (d, J = 7.5 Hz, 2H).), 7.83 (d, J = 7.1 Hz, 2H), 7.69 (m, 8H), 7.56 (s, 2H), 6.99 (s, 4H), 6.96 (s, 2H), 6.90 (s, 2H), 6.41 (s, 4H), 3.87 (t, J = 6.2 Hz, 8H). 1.71–1.67 (m, 8H), 1.35–1.19(m, 42H), 0.80 (t, J = 6.7 Hz, 12H). ^{13}C NMR (101 MHz, $CDCl_3$) δ (ppm): 188.30, 160.31, 158.81, 154.05, 153.10, 149.66, 148.24, 147.45, 147.08, 140.45, 139.99, 138.18, 137.12, 137.05, 136.80, 134.99, 134.65, 134.35, 134.02, 125.16, 123.62, 122.78, 121.89, 120.21, 115.53, 114.66, 114.63, 114.13, 110.54, 68.92, 68.33, 63.40, 31.95, 31.78, 29.91, 29.70, 29.67, 29.63, 29.58, 29.46, 29.41, 29.37, 29.18, 26.07, 22.72, 22.61, 14.15, 14.05.

3. Results and discussion

The synthesis route of DTF-IC is shown in Scheme 1 and the detailed procedures of experiments are shown in Figs. S1 and S2 (online). Compound 1 was synthesized according to references [29]. The target molecule DTF-IC was prepared via Stille coupling of compound **1** and compound **2**. The twin spiro structures in molecular structure could increase the steric hindrance, thereby affecting the aggregation morphology of the molecule. DTF-IC energy level was measured by electrochemical cyclic voltammetry (*CV)* method as shown in Fig. S3 (online) [30]. The thermal stability of DTF-IC was measured using thermo gravimetric analysis (TGA). From Fig. S4 (online), it can be observed that DTF-IC has a decomposition temperature (T_d) at 340 °C, so the SM DTF-IC displays fair thermal stability. As can be seen from Fig. 1b, HOMO level of DTF-IC is −5.54 eV and LUMO level is −3.86 eV, which are between the corresponding energy levels of PBDB-T and IT-M. These cascade energy levels increased the charge transfer channel, which reduced charge recombination. In addition to the matched energy levels, it can be observed from the normalized absorption spectra of single-component films of the PBDB-T, IT-M, and DTF-IC (Fig. 1c) that the absorption peak position of PBDB-T was 634 nm, the absorption peak of IT-M was 711 nm, while the third component of DTF-IC was 746 nm, which just filled the gap in the binary system to give the absorption spectrum of the acceptor at 650–690 nm and broaden the absorption in the range of 730–830 nm. With the addition of DTF-IC, the photon acquisition was greatly enhanced. Based on the absorption spectrum of PBDB-T:IT-M:DTF-IC blend films (Fig. 1d), the overall absorption intensity of ternary films in the visible region was indeed higher than that of the binary films. This extended the absorption spectrum so that the active layer could absorb more sunlight and produce more excitons, which was the crucial factor for boosting short-circuit current.

In order to explore the photovoltaic performance of DTF-IC, a series of organic solar cells was prepared using PBDB-T: IT-M: DTF-IC as the active layer [31]. The device structure is shown in Fig. 2a: ITO/PEDOT:PSS/active layer/PDINO/Al. The weight ratio between the donor and acceptor was kept fixed at 1:1, and the ratios of DTF-IC and IT-M were constantly changed to achieve different doping ratios. Since the solubility of DTF-IC in chlorobenzene was not as good as in chloroform, DTF-IC was firstly dissolved in chloroform and then added to the chlorobenzene solution of the active layer in different proportions. To achieve the best device performance, DTF-IC of 0%, 10%, 20%, 30%, 50% and 100% were added into the active layer to explore the power conversion efficiency, respectively. The *J-V* curve of the device was measured under AM 1.5G, 100 mW/cm^2. Referring to Fig. 2b, with the increase of DTF-IC ratio, the J_{sc} keeps increasing continuously in an appropriate range, while FF remains relatively stable. When the doping ratio reached 10%, the device had the best performance and the J_{sc} reached the highest value of 17.95 mA/cm^2, the V_{oc}

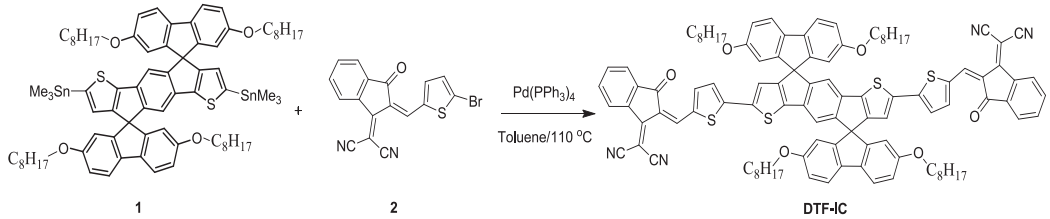

Scheme 1. Synthetic route of DTF-IC.

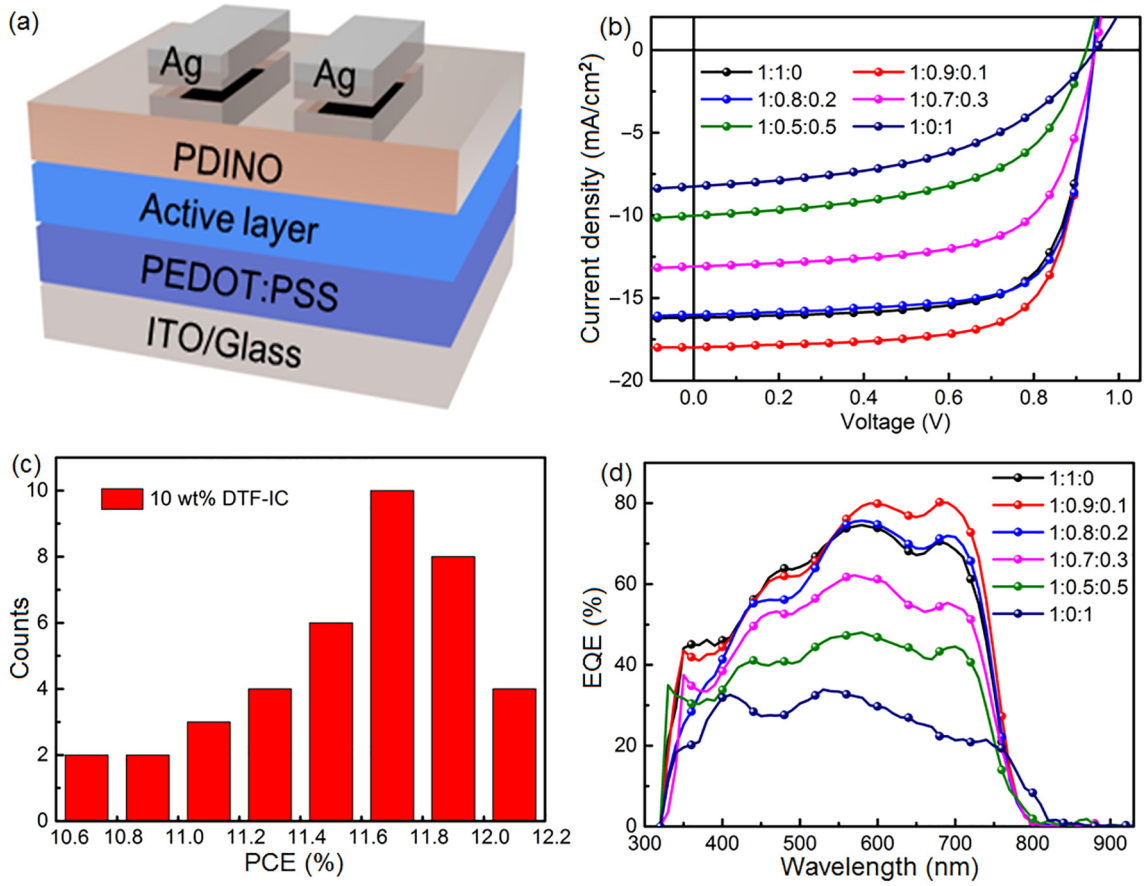

Fig. 2. (Color online) Ternary organic solar cells with 12.14% PCE. (a) Schematic diagram of the device structure, (b) *J-V* curves of OSCs with different DTF-IC contents, (c) PCE histogram based on 39 ternary OSCs with 10 wt% DTF-IC in acceptors, (d) EQE spectra of the corresponding OSCs.

reached 0.94 V, and the PCE was 12.14%. This was due to the addition of DTF-IC which widened the absorption spectrum of the active layer, and the cascade of energy contributed to charge transport and energy transfer, facilitating the generation and dissociation of excitons and the collection of charge in the active layer. When the doping ratio reached 20%, the PCE could still be maintained at 11%. However, when the ratio of DTF-IC was further increased, chlorobenzene and chloroform solution did not have a good miscibility with one another, which results to poor morphology of the film induced by the damage in charge transfer pathway between PBDB-T and IT-M. Consequently, the charge transfer process was severely hindered and thus, causing the significant drop in current and fill factor. The main photovoltaic parameters are summarized in Table 1. To further confirm the effect of adding 10% DTF-IC, data verification from 39 identical devices in different batches was performed and the statistical distribution histogram of power conversion efficiency was calculated. It can be seen from Fig. 2c that the power conversion efficiency doped with 10% DTF-IC is mostly distributed above 11.8%, which is generally higher than that of binary devices. The change of J_{sc} can be explained not only from the absorption spectrum of the film, but also from the external quantum efficiency (EQE) spectrum of ternary organic solar cell. To further illustrate the important contribution of J_{sc} in power conversion efficiency, the measurement of EQE had also been used to demonstrate the advantages of introducing DTF-IC. Based on Fig. 2d, DTF-IC broadens the spectrum absorption between 650 and 750 nm, the EQE value increases to varying degrees with the addition of DTF-IC in this region. It was clear that when the doping ratio was 10%, the addition of DTF-IC filled the gap between the absorption peaks of PBDB-T and IT-M in the range of 650–690 nm to the greatest extent, which improved the utilization of exciton in this range and maximized the absorption, so that the J_{sc} value shown in the EQE diagram could reach up to 20 mA/cm^2. However, with the increase of DTF-IC, the reduction of IT-M ratio reduced the harvesting of short-wavelength photons by the active layer. It was also possible that the larger doping ratio of DTF-IC destroys the morphology of the active layer. The exciton dissociation in the active layer and the carrier transport or collection was reduced for larger DTF-IC doping ratio. Similarly, the EQE value also dropped in the larger DTF-IC doping ratio, consistent with the decreasing trend of J_{sc} with increasing DTF-IC doping.

To study the exciton kinetics between the two acceptors in the blend film, the PL spectra of the blended film and the corresponding solution were characterized under the same conditions. It can be seen from Fig. S5 (online) that PBDBT, DTF-IC, and ITM films exhibit clear PL spectra. The DTF-IC and ITM can almost quench PL spectrum of PBDBT. Fig. 3a shows the PL spectrum of acceptors doped with different DTF-IC. The emission peak of IT-M was obviously strong, while the emission peak of DTF-IC was relatively weak. Nonetheless, it can be concluded clearly that the emission intensity of IT-M decreases significantly with the increases of DTF-IC doping ratio. When doped with 10%, the emission had been mostly suppressed, indicating that most of excitons were effectively dissociated at the IT-M:DTF-IC interface or most of the energy was transferred from IT-M to DTF-IC. Since the cascade energy level structure reduced the barrier of charge transfer in the active layer, effective exciton dissociation and carrier transport or collection were expected. To further verify whether efficient energy transfer had occurred, characterization of the PL spectrum of the blended solution doped with different ratios of DTF-IC were

Table 1
The photovoltaic parameters for PBDB-T:IT-M:DTF-IC devices under simulated AM 1.5G illumination at 100 mW/cm^2.

DTF-IC content (wt%)	V_{oc} (V)	J_{sc} (mA/cm^2)	J_{cal} (mA/cm^2)[a]	FF	PCE_{max} (%) $PCE_{avg.}$ (%)[b]
0	0.94	16.18	15.62	0.71	10.90/10.76
10	0.94	17.95	17.35	0.72	12.14/11.76
20	0.95	15.86	15.33	0.73	11.04/10.84
30	0.94	13.08	12.98	0.66	8.16/8.12
50	0.92	10.56	10.42	0.56	5.16/5.03
100	0.94	8.23	7.86	0.48	3.75/3.68

[a] J_{cal} was calculated from EQE spectra.
[b] The average was obtained from over 30 devices.

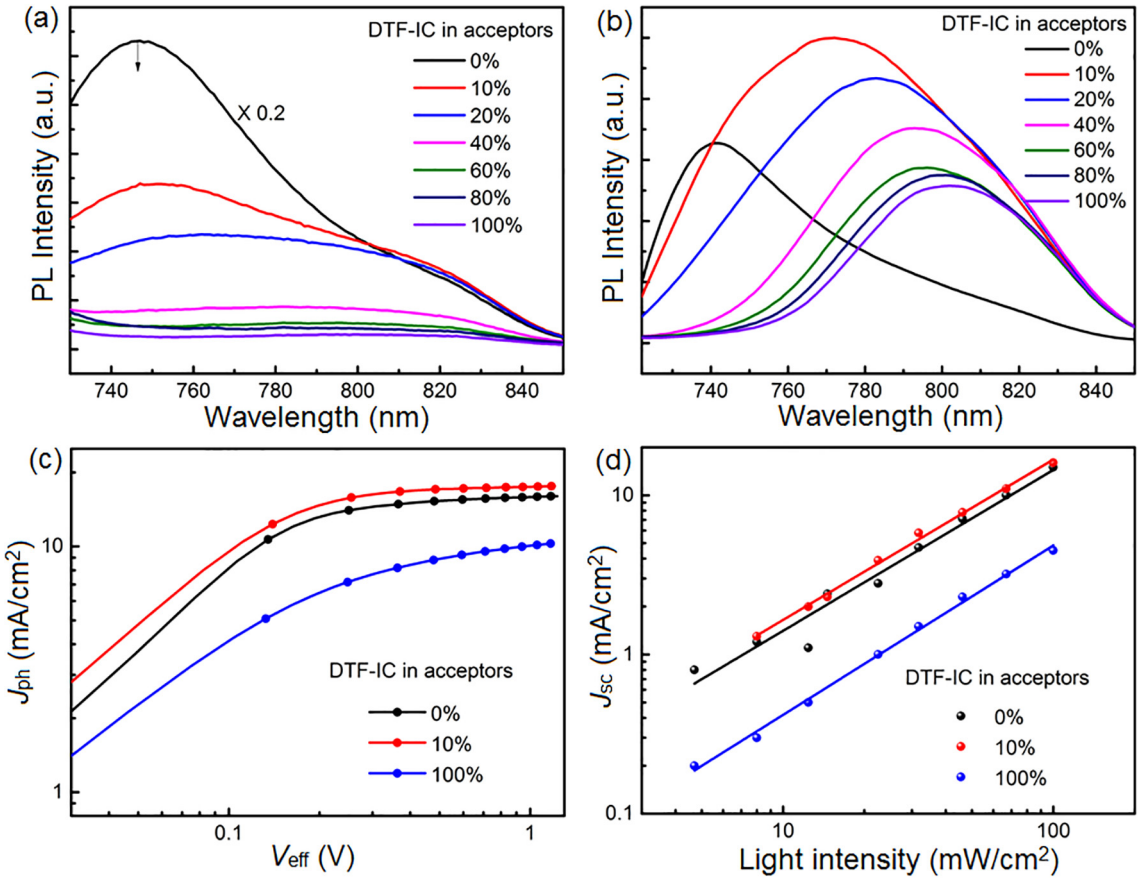

Fig. 3. (Color online) PL spectra, J_{sc}-P_{light} and J_{ph}-V_{eff} curves of ternary devices. (a) PL spectra of neat IT-M, DTF-IC and blend IT-M: DTF-IC films and (b) blend solution under 712 nm light excitation. (c) Photocurrent density versus effective voltage characteristics. (d) Dependence of J_{sc} on light intensity for the ternary OSCs with different DTF-IC contents.

conducted (Fig. 3b) [32,33]. Pure IT-M had a strong emission in the range of 730–750 nm, and the emission peak was 740 nm; pure DTF-IC had strong emission in the range of 790–810 nm, and the emission peak was 800 nm. With the addition of DTF-IC in the IT-M solution, the PL emission of IT-M was obviously quenched, and the PL at 780–800 nm was gradually enhanced. Furthermore, it was observed that the PL intensity of IT-M:DTF-IC blend solution was higher than that of pure DTF-IC solution under the same excitation wavelength of 712 nm. Both of these illustrate that the energy on IT-M can be efficiently transferred to DTF-IC [34]. However, charge transport still relies primarily on the charge transport channels formed by the host system. Hence, when the proportion of the third component exceeds 20%, a charge trap will be formed, and higher doping ratio will also cause significant reduction in J_{sc} and FF of the device.

To gain deeper understanding of the generation, dissociation and charge collection of excitons in the active layer, the relationship between the photocurrent density J_{ph} and the effective voltage V_{eff} [35] was studied as displayed, as shown in Fig. 3c. According to the theory: $J_{ph} = J_L - J_D$, that is, the photocurrent minus the dark current, and $V_{eff} = V_0 - V_a$, where V_0 is the value of V_a when $J_{ph} = 0$. Exciton dissociation and charge collection efficiency $P(E, T) = J_{ph}/J_{sat}$ [36,37]. According to this formula, the exciton dissociation was calculated to be 0.991, 0.995, and 0.890 for devices doped with 0%, 10%, and 100% DTF-IC, respectively. $P(E, T)$ close to 1 illustrates that it can facilitate charge collections and extractions. It could be deduced that the device with 10% DTF-IC had the best performance. This was due to cascaded distribution of energy level between DTF-IC and IT-M, which promoted the charge transport and collection process. In order to explore the molecular recombination mechanism, the *J-V* curves of the OSCs under different light intensities were studied (Fig. 3d). The correlation between J_{sc} and P_{light} (light intensity) can be fitted to the equation: $J_{sc} \propto P^{\alpha}$ [38]. When $\alpha = 1$, bimolecular recombination can be

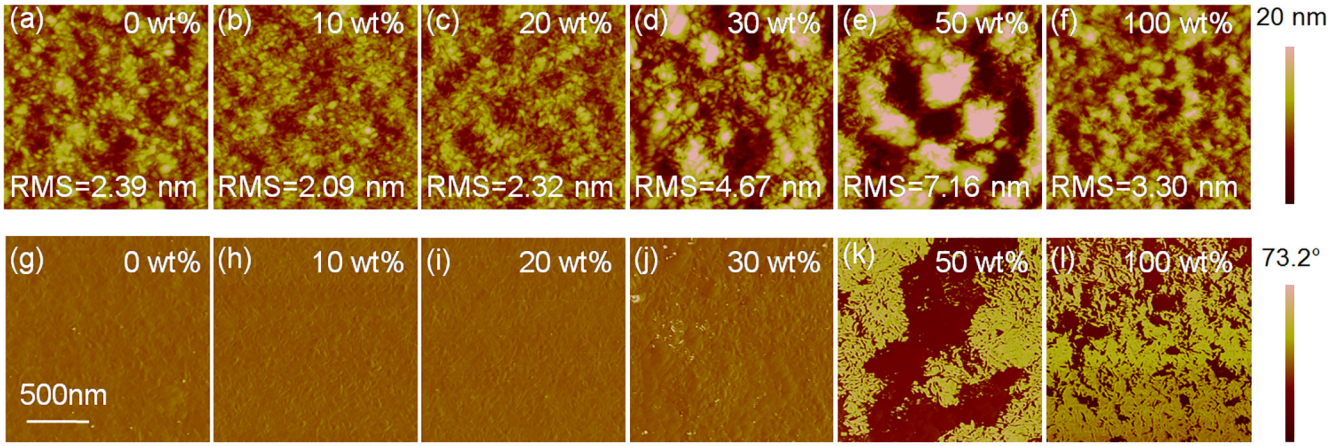

Fig. 4. (Color online) $2 \times 2\ \mu m^2$ AFM height (upper) and phase (lower) images of ternary blends with different content of DTF-IC.

neglected, and when α is closed to 1, fewer charge-recombination happened. It can be seen from Fig. 2d that α value of the binary device is 1.010, and the value of the ternary device with 10% DTF-IC is 1.007, indicating that the addition of appropriate amount of DTF-IC can effectively inhibit the bimolecular recombination. This was mainly because of the proper amount of DTF-IC that caused the active layer to form a phase-separated structure of appropriate size and optimized the crystallization process of the active layer. It is beneficial to promote a good morphology for better charge extraction and minimal charge recombination. To investigate the effect of different DTF-IC contents on the charge transport of the active layer, the charge transport and extraction properties were studied. The space-charge-limited-current (SCLC) method was used to measure the mobility of electrons and holes in the device, as shown in Fig. S6 (online) [39]. The device structure of hole-only was ITO/PEDOT:PSS/active layer/MoO_3/Al, and the device structure of electron-only was ITO/Al/active layer/PDINO/Al. The $J^{0.5}$-V curve is shown in Figs. S7 and S8 (online). From the mobility image, the trend of electron mobility was 5.36×10^{-4}, 6.63×10^{-4}, 4.63×10^{-4}, 1.95×10^{-4}, 5.04×10^{-5}, and 3.74×10^{-6}cm^2/(V s), the change trend of hole mobility was 2.14×10^{-4}, 2.48×10^{-4}, 1.74×10^{-4}, 8.23×10^{-5}, 1.95×10^{-5}, and 2.89×10^{-6}c cm^2/(V s). DTF-IC doped with 10% increased the electron mobility and hole mobility compared to the binary device, when the doping ratio was greater than 10%, the trapped state density was increased as the excess DTF-IC destroyed the charge transport channel, thus, affecting the transmission and collection of charge and reducing the charge mobility.

The surface topography of binary and ternary films were characterized by atomic force microscopy (AFM) [40] to further investigate the effect of DTF-IC doping ratio on the FF of the device. Fig. 4 is a height and phase diagram of PBDB-T:IT-M:DTF-IC film doped with different weight ratios. Based on Fig. 4, the root-mean-square (RMS) roughness of the ternary film doped with 0%, 10%, 20%, 30%, 50% and 100% was 2.39, 2.09, 2.32, 4.67, 7.16, and 3.30 nm, respectively. Compared with PBDB-T:IT-M film, the surface of PBDB-T:IT-$M_{0.9}$: DTF-$IC_{0.1}$ film was relatively smooth, which was due to the strong crystallinity nature of DTF-IC that could accelerate the phase separation between the acceptors. The premise of this conclusion is that DTF-IC does have strong crystallinity, as shown in Fig. S9 (online). The pure DTF-IC film exhibited two obvious diffraction peaks located at (6.13°) and (21.15°), corresponding to a lamellar distance of (14.41 Å) and a $\pi-\pi$ stacking distance of (4.19 Å), respectively. This obvious diffraction peak indicates that DTF-IC has strongly crystalline. Such proper phase separation was conducive for exciton dissociation and carrier transport and collection, thereby increasing J_{sc} and FF. However, when the doping of the third component exceeded a certain ratio, the surface experienced a sharp increase in roughness as shown from the height diagram, which might be attributed to the strong crystalline nature of DTF-IC, resulting in a strong aggregation that occurred in the blend film. This destroyed the interpenetrating network structure of PBDB-T:IT-M main system. The results of surface morphology were consistent with the photovoltaic performance of the device.

4. Conclusion

In conclusion, a novel non-fullerene small-molecular acceptor DTF-IC had been developed to introduce in PBDB-T:IT-M system as a third component. The power conversion efficiency of PBDB-T:IT-M: DTF-IC increased to 12.14% when the content of DTF-IC was 10%. The PCE improvement was attributed to the substantial enhancement of J_{sc}, and the increased J_{sc} was caused by the broader absorption of the active layer on the range of 730–800 nm due to the introduction of DTF-IC. Moreover, the introduction of the third component provided a cascaded energy between donor and acceptor and reduced the charge transfer barrier in the active layer. The effective charge transfers between the double acceptors promoted dissociation of excitons and the collection of carriers. Meanwhile, efficient energy transfer between the non-fullerene acceptors could enhance charge transport and reduce charge recombination as well. The charge recombination was suppressed while the J_{sc} was greatly increased, which could increase the FF slightly. This was because the high crystallinity of DTF-IC could optimize the crystallization process of active layer while maintaining proper phase separation, thereby obtaining an efficient ternary solar cell. This work further demonstrates that ternary organic solar cells are one of the best candidates for organic photovoltaic industrialization.

Conflict of interest

The authors declare that they have no conflict of interest.

Acknowledgments

This work was supported by the Startup Funding of Hebei University of Technology (208011), the National Key R&D Program of China (2017YFE0106000), the National Natural Science Foundation of China (51773212, 21574144, and 61705240), Zhejiang Provincial Natural Science Foundation (LR16B040002), Ningbo Municipal Science and Technology Innovative Research

Team (2015B11002 and 2016B10005), CAS Interdisciplinary Innovation Team, CAS Key Project of Frontier Science Research (QYZDB-SSW-SYS030) and CAS Key Project of International Cooperation (174433KYSB20160065).

Author contributions

Lirong Wu and Lingchao Xie conceived the idea and designed the experiments. Jiaming Huang, Ruixiang Peng, Wei Song and Songting Tan analyzed the experimental data. Billy Fanady and Hanmin Tian polished the article. Lirong Wu and Lingchao Xie wrote the paper. Wengang Bi and Ziyi Ge supervised the project.

Appendix A. Supplementary data

Supplementary data to this article can be found online at https://doi.org/10.1016/j.scib.2019.06.008.

References

[1] Fu H, Wang Z, Sun Y. Advances in non-fullerene acceptor based ternary organic solar cells. Solar RRL 2018;2:1700158.
[2] Yang L, Yan L, You W. Organic solar cells beyond one pair of donor-acceptor: ternary blends and more. J Phys Chem Lett 2013;4:1802–10.
[3] Yu R, Yao H, Hou J. Recent progress in ternary organic solar cells based on nonfullerene acceptors. Adv Energy Mater 2018;8:1702814.
[4] An Q, Ma X, Gao J, et al. Solvent additive-free ternary polymer solar cells with 16.27% efficiency. Sci Bull 2019;64:504–6.
[5] Zheng Z, Hu Q, Zhang S, et al. A highly efficient non-fullerene organic solar cell with a fill factor over 0.80 enabled by a fine-tuned hole-transporting layer. Adv Mater 2018;30:e1801801.
[6] Cheng P, Wang R, Zhu J, et al. Ternary system with controlled structure: a new strategy toward efficient organic photovoltaics. Adv Mater 2018;30:1705243.
[7] Cui Y, Zhang S, Liang N, et al. Toward efficient polymer solar cells processed by a solution-processed layer-by-layer approach. Adv Mater 2018;30:e1802499.
[8] Zhang K, Xia R, Fan B, et al. 11.2% All-polymer tandem solar cells with simultaneously improved efficiency and stability. Adv Mater 2018;30:e1803166.
[9] Zhou Z, Xu S, Song J, et al. High-efficiency small-molecule ternary solar cells with a hierarchical morphology enabled by synergizing fullerene and non-fullerene acceptors. Nat Energy 2018;3:952–9.
[10] Zhong L, Gao L, Bin H, et al. High efficiency ternary nonfullerene polymer solar cells with two polymer donors and an organic semiconductor acceptor. Adv Energy Mater 2017;7:1602215.
[11] Zhao F, Li Y, Wang Z, et al. Combining energy transfer and optimized morphology for highly efficient ternary polymer solar cells. Adv Energy Mater 2017;7:1602552.
[12] Zhang H, Wang X, Yang L, et al. Improved domain size and purity enables efficient all-small-molecule ternary solar cells. Adv Mater 2017;29:1703777.
[13] Xie Y, Yang F, Li Y, et al. Morphology control enables efficient ternary organic solar cells. Adv Mater 2018;30:e1803045.
[14] Xiao B, Tang A, Zhang J, et al. Achievement of high V_{oc} of 1.02 V for P3HT-based organic solar cell using a benzotriazole-containing non-fullerene acceptor. Adv Energy Mater 2017;7:1602269.
[15] Xiao B, Tang A, Yang J, et al. P3HT-based photovoltaic cells with a high V_{oc} of 1.22 V by using a benzotriazole-containing nonfullerene acceptor end-capped with thiazolidine-2,4-dione. ACS Macro Lett 2017;6:410–4.
[16] Tang A, Xiao B, Wang Y, et al. Simultaneously achieved high open-circuit voltage and efficient charge generation by fine-tuning charge-transfer driving force in nonfullerene polymer solar cells. Adva Funct Mater 2018;28:1704507.
[17] Tang A, Xiao B, Chen F, et al. The introduction of fluorine and sulfur atoms into benzotriazole-based p-type polymers to match with a benzotriazole-containing n-type small molecule: "the same-acceptor-strategy" to realize high open-circuit voltage. Adv Energy Mater 2018;8:1801582.
[18] Li T, Wang J, Chen H, et al. Nonfullerene acceptor with strong near-infrared absorption for polymer solar cells. Dyes Pigments 2017;137:553–9.
[19] Wang C, Xu X, Zhang W, et al. Ternary organic solar cells with enhanced open circuit voltage. Nano Energy 2017;37:24–31.
[20] Zhang G, Zhang K, Yin Q, et al. High-performance ternary organic solar cell enabled by a thick active layer containing a liquid crystalline small molecule donor. J Am Chem Soc 2017;139:2387–95.
[21] Jiang W, Yu R, Liu Z, et al. Ternary nonfullerene polymer solar cells with 12.16% efficiency by introducing one acceptor with cascading energy level and complementary absorption. Adv Mater 2018;30:1703005.
[22] Nian L, Kan Y, Wang H, et al. Ternary non-fullerene polymer solar cells with 13.51% efficiency and a record-high fill factor of 78.13%. Energy. Environ Sci 2018;11:3392–9.
[23] An Q, Zhang F, Gao W, et al. High-efficiency and air stable fullerene-free ternary organic solar cells. Nano Energy 2018;45:177–83.
[24] Zhang G, Zhao J, Chow PCY, et al. Nonfullerene acceptor molecules for bulk heterojunction organic solar cells. Chem Rev 2018;118:3447–507.
[25] Gasparini N, Salleo A, McCulloch I, et al. The role of the third component in ternary organic solar cells. Nat Rev Mater 2019;4:229–42.
[26] Zhang J, Tan HS, Guo X, et al. Material insights and challenges for non-fullerene organic solar cells based on small molecular acceptors. Nat Energy 2018;3:720–31.
[27] Li S, Ye L, Zhao W, et al. Energy-level modulation of small-molecule electron acceptors to achieve over 12% efficiency in polymer solar cells. Adv Mater 2016;28:9423–9.
[28] Zhang S, Qin Y, Zhu J, et al. Over 14% efficiency in polymer solar cells enabled by a chlorinated polymer donor. Adv Mater 2018;30:e1800868.
[29] Xie L, Xiao J, Wu L, et al. Synthesis and photovoltaic properties of small molecule electron acceptors with twin spiro-type core structure. Dyes Pigments 2019;168:197–204.
[30] Yao H, Chen Y, Qin Y, et al. Design and synthesis of a low bandgap small molecule acceptor for efficient polymer solar cells. Adv Mater 2016;28:8283–7.
[31] Li W, Ye L, Li S, et al. A high-efficiency organic solar cell enabled by the strong intramolecular electron push-pull effect of the nonfullerene acceptor. Adv Mater 2018;30:e1707170.
[32] Gupta V, Bharti V, Kumar M, et al. Polymer-polymer forster resonance energy transfer significantly boosts the power conversion efficiency of bulk-heterojunction solar cells. Adv Mater 2015;27:4398–404.
[33] Goh T, Huang JS, Bielinski EA, et al. Coevaporated bisquaraine inverted solar cells: enhancement due to energy transfer and open circuit voltage control. ACS Photon 2015;2:86–95.
[34] Huang J-S, Goh T, Li X, et al. Polymer bulk heterojunction solar cells employing Förster resonance energy transfer. Nat Photon 2013;7:479–85.
[35] Lenes M, Morana M, Brabec CJ, et al. Recombination-limited photocurrents in low bandgap polymer/fullerene solar cells. Adv Funct Mater 2009;19:1106–11.
[36] Peng R, Liu Z, Guan Q, et al. Highly efficient non-fullerene polymer solar cells enabled by novel non-conjugated small-molecule cathode interlayers. J Mater Chem A 2018;6:6327–34.
[37] Lee J, Sin DH, Moon B, et al. Highly crystalline low-bandgap polymer nanowires towards high-performance thick-film organic solar cells exceeding 10% power conversion efficiency. Energy Environ Sci 2017;10:247–57.
[38] Schilinsky P, Waldauf C, Brabec CJ. Recombination and loss analysis in polythiophene based bulk heterojunction photodetectors. Appl Phys Lett 2002;81:3885–7.
[39] Guan Q, Peng R, Liu Z, et al. Highly efficient polymer solar cells employing natural chlorophyllin as a cathode interfacial layer. J Mater Chem A 2018;6:464–8.
[40] Mimura M, Tanaka H. Long-term performance of a generic intrusion detection method using doc2vec. 2017. In: Fifth International Symposium on Computing and Networking (CANDAR), 2017. p. 456–62.

Lirong Wu received her B.S. degree in Electronic Science and Technology from Hebei University of Science and Technology in 2017. Now she is a M.S. student at Hebei University of Technology under the supervision of Dr. Wengang Bi. Since July 2018, she has been working in Ziyi Ge Group at Ningbo Institute of Materials Technology and Engineering as a visiting student. Her research interests focus on the device of organic solar cells.

Lingchao Xie received his B.S degree in Applied Chemistry from College of Chemistry, Xiangtan University in 2016. Now he is pursuing his M.S. degree under the supervison of Prof. Songting Tan in College of Chemistry, Polymer Chemistry and Physics at Xiangtan University and works under the joint supervision of Prof. Ziyi Ge at Ningbo Institute of Materials Technology and Engineering. His research interest focuses on the synthesis and application of organic photovoltaic materials.

Wengang Bi received his Ph.D. degree from Department of Electrical and Computer Engineering, University of California, San Diego, in 1997. After devoting his career on forefront research and development at Hewlett Packard Laboratories, Agilent Technologies Inc., and Philips-Lumileds, Dr. Bi currently works at Hebei University of Technology as a distinguished professor. His research interests include GaN-based semiconductor materials and devices, colloidal quantum dots and their applications to lighting, display and solar cells.

Ziyi Ge got the Ph.D. degree in Institute of Chemistry, Chinese Academy of Sciences. He conducted his postdoctoral research of organic electronics in Tokyo Institute of Technology, Kanagawa University, Japan and the University of New South Wales, Australia. Currently, he is the leader of Organic Electronic Material and Device Group at Ningbo Institute of Material Technology and Engineering, Chinese Academy of Sciences. His research interests focus on OLEDs, organic solar cells, and the related materials.